Nuclear Engineering and Design 367 (2020) 110780

Contents lists available at ScienceDirect

Nuclear Engineering and Design

journal homepage: www.elsevier.com/locate/nucengdes

Effect of condenser tube inclination on the flow dynamics and instabilities in a passive containment cooling system (PCCS) for nuclear safety

Michel Haag, P. Karthick Selvam*, Stephan Leyer

Faculty of Science, Technology and Medicine, Department of Engineering, Campus Kirchberg, University of Luxembourg, 6, rue Richard Coudenhove-Kalergi, L-1359 Kirchberg, Luxembourg

ARTICLE INFO

Keywords:
External condenser PCCS
Flashing
Geysering
Mass flow excursion
Pool stratification
Experimental facility

ABSTRACT

The release of steam into the containment of a nuclear plant during accidents (e.g. Fukushima) impose tremendous thermal and pressure load on the structure. Passive Containment Cooling Systems (PCCS) are heat exchangers designed to remove and transfer heat using natural forces (e.g. buoyancy, gravity) from the containment to protect its structural integrity. Depending on the design, the heat sink is usually a water pool or ambient air circulating around the steel containment structure. The presented work deals with the external condenser PCCS design where steam condenses on the external surface of a condense tubes in the containment. The heat sink is an overhead water pool and flow circulation occurs via the downcomer and riser tubes connected to either side of the condenser tube.

The first part of this work provides an overview of the existing literature on external condenser PCCS highlighting a major shortcoming – the influence of the condenser tube inclination on the resulting flow dynamics within the downcomer and riser tubes has not yet been investigated. The second part of this work discusses the INTRAVIT (Investigation of passive heat Transfer in a Variably Inclined Tube) test facility setup at the University of Luxembourg to address the aforementioned shortcoming. The condenser tube inclination in the INTRAVIT facility could be adjusted between 0° (horizontal) and 90° (vertical) making it possible to quantitatively assess the different flow phenomena (e.g. mass flow excursions, boiling, flashing, geysering etc.) taking place in the downcomer, condenser and riser tubes at different inclinations. An important feature of the facility is the easy adjustment of pool temperature to perform tests at different starting temperatures.

In the final part of this work, results from 6 tests conducted using a combination of two different pool temperatures (50 °C and 85 °C) and three condenser tube inclinations (5°, 60°, and 90°) are discussed. Temperature, local void fraction, and flow rate data from thermocouples, needle probes, and mass flow sensors provide a detailed description of the stable single phase and highly unstable two-phase flow behavior observed during the tests.

1. Introduction

The Fukushima-Daiichi nuclear power plant (NPP) accident in 2011 highlighted the main limitation of active cooling systems used to remove decay heat from the reactor core after its shutdown – their reliance on electrical power for operation. Research on passive safety systems (PSS) relying on natural forces (e.g. gravity, buoyancy) for its operation was already underway pre-Fukushima (IAEA, 1991a) and has since rapidly accelerated post-Fukushima. Reliable operation in the absence of electrical power, simplification of plant design leading to better performance and improved economics are the main features of passive safety systems. A clear description of the criterion to classify something as active and passive safety systems is provided in IAEA (1991b). A summary of thermal–hydraulic phenomena (e.g. stratification, condensation, natural convection and circulation, pressure drop etc.) during the operation of PSS in water-cooled reactors (e.g. AP1000, ESBWR, WWER-1000/392 etc.) and integral reactor systems (e.g. SMART, CAREM, MASLWR, IRIS etc.) is summarized in IAEA (2009).

From the standpoint of NPP design, the containment acts as the final barrier in preventing the release of radioactive substances to the atmosphere. During a loss of coolant accident (LOCA), release of steam and other gases could over-pressurize the containment beyond its design limit posing a risk to its structural integrity. Such safety concerns have led to the development of Passive containment cooling systems (PCCSs) that are designed to protect the containment during accidents. It is a PSS operating on the principle of natural circulation to remove

* Corresponding author.
E-mail address: karthick.selvam@uni.lu (P.K. Selvam).

https://doi.org/10.1016/j.nucengdes.2020.110780
Received 30 October 2019; Received in revised form 6 May 2020; Accepted 20 July 2020
Available online 29 July 2020

Nomenclature

α	Inclination angle
P	Power
T	Temperature
TUP	Temperature upper pool

Abbreviations

ABWR	Advanced boiling water reactor
AHWR	Advanced heavy water reactor
AP	Advanced Passive
CAREM	Central ARgentina de Elementos Modulares
ESBWR	Economic simplified boiling water reactor
HET	Heat exchanger tubes
HPR1000	Hualong Pressurised Reactor
INTRAVIT	Investigation of passive heat transfer in a variably inclined tube
iPOWER	Innovative power reactor
IRIS	International Reactor Innovative and Secure
LOCA	Loss of coolant accident
LSBWR	Long operation cycle simplified boiling water reactor
MASLWR	Multi-Application Small Light Water Reactor
NPP	Nuclear power plant
PCCS	passive containment cooling system
RMWR	Reduced moderation water reactor
SMART	System-integrated modular advanced reactor
SWR	Siedewasserreaktor (engl. boiling water reactor)
WWER	Water-water energetic reactor

heat and condense steam to maintain the containment pressure level within design limits acting as the ultimate heat sink. An illustration of the two predominant PCCS designs is shown in Fig. 1.

(i) The first (Type-I) design enables heat transfer between a containment (made of concrete) and an overhead water pool. Two prominent variations exist (Jeon et al., 2015a, Jeon et al., 2015b) in this design depending on the location of steam condensation. One is termed 'external condenser' if steam condenses on the outer surface of the condenser tubes placed near the top of the containment. This is used in the KERENA (formerly SWR1000) (Stosic et al., 2008), AHWR (Sinha and Kakodkar, 2006; Kakodkar, 2014), HPR1000 (Xing et al., 2016), iPower (Lee et al., 2017), and WWER-1200 (Bakhmet'ev et al., 2009; Bezlepkin et al., 2014) reactors. Another is termed 'internal condenser' if steam condenses inside the condenser tubes. This is used in the ABWR-II, RMWR, ESBWR, and LSBWR reactors (IAEA, 2009).

(ii) The second (Type-II) PCCS (Fig. 1(c)) design uses a conductive containment wall (e.g. steel) to transfer heat from the inner surface of the primary containment wall to the air and/or water flow on its outer surface. This design is incorporated in the AP600 (Tower et al., 1988) and AP1000 (Schulz, 2006) reactors.

The focus of this work is to study the flow and heat transfer dynamics of the secondary coolant side in an external condenser PCCS under different condenser tube inclinations. Given below is the description of the external condenser PCCS operation that is necessary to understand the objective of the research presented in this study.

Steam released during a LOCA as well as after a containment isolation causes a rise in the containment pressure. Fluid (typically water) inside the condenser tubes begins absorbing heat from steam activating the PCCS operation. The heated fluid moves upward via long riser tubes into an overhead shielding/storage pool due to buoyancy. Concurrently, gravity brings down the cold fluid via downcomer tubes into the condenser tubes for the natural circulation to continue as illustrated in Fig. 2. This phenomenon reduces the containment pressure providing grace period for the operators and decision makers. After many hours in operation, fluid in the loop (pool, downcomer-, condenser-, and riser-tubes) attain near saturation temperatures. Now as the fluid gets heated and ascends upward in the riser tube, a reduction in static pressure causes sudden fluid evaporation at a certain height resulting in a violent motion of the vaporized mass into the pool. This phenomenon is termed 'Flashing'.

At the same instant during flashing in the riser tube, the downcomer tube experiences a similar downward surge in fluid mass flow. This instability in the flow caused by flashing subsides after a short while and single-phase flow condition is restored. The fluid gets heated again in the condenser tube and starts flashing again during its ascent in the riser tube. This cycle is repeated at regular intervals. After many flashing cycles, the fluid starts boiling in the condenser tube and evaporates much early in the riser tube resulting in a flashing-like phenomenon termed 'Geysering'. The geysering cycle is now repeated at regular intervals dictating the flow and heat transfer dynamics within the PCCS. Both flashing and geysering greatly affect the overall flow stability within the PCCS loop resulting in rapid transients that might, at times, lead to water hammer effects (Hou et al., 2016).

2. Literature review

One of the early external condenser PCCS experiments was carried out at the PANDA (Passive Nachwärmeabfuhr und Druckabbau Test Anlage) facility at PSI, Switzerland (Dreier et al., 1999) to assess its performance for the SWR 1000 (now KERENA) reactor. Tests characterizing different accident scenarios are done to assess the behavior of different passive safety systems including the PCCS. It is observed that the PCCS pool temperature gradually increased during the tests before

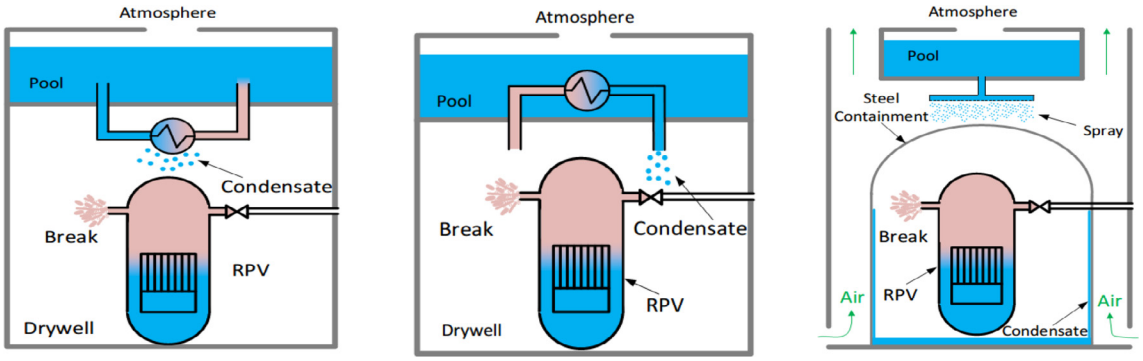

Fig. 1. Type-I PCCS (a) external condenser, and (b) internal condenser design; (c) Type-II PCCS.

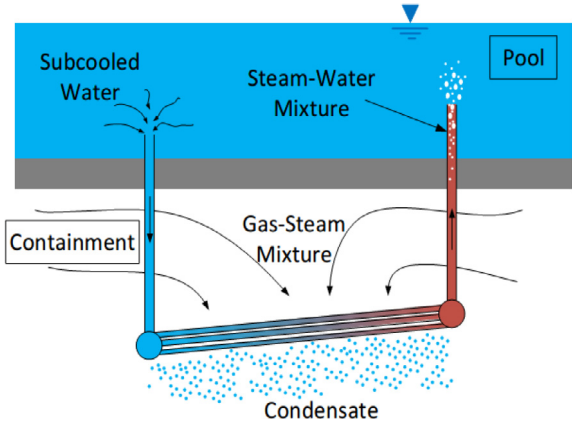

Fig. 2. Illustration of the external condenser PCCS.

attaining saturation conditions where the transition from single- to two-phase flow natural circulation occurred. This is accompanied by flow oscillations in the feed and return lines of the PCCS.

Liu et al. (2000) performed steam condensation tests in the presence of non-condensable gases (e.g. air, helium) to evaluate the primary side heat removal capacity of two PCCS designs with a vertical riser tube, namely, (i) the thermosyphon loop, and (ii) internal evaporator only (IEO) system. Tests are conducted at varying pressures (2.48–4.55 bar) and air mass fraction (0.3–0.65). Results showed that condensation heat transfer coefficients are lower when helium is introduced leading to gas stratification phenomenon as the helium mole fraction exceeds 60%.

Manera et al. (2005) performed natural and forced convection experiments at the CIRCUS facility using water/steam as the working fluid to assess the start-up phase of a natural circulation cooled boiling water reactor (BWR). Tests are performed in the pressure and temperature range of 1–5 bar and 70–90 °C, respectively. Advanced wire mesh sensor (WMS) instrumentation installed in the vertical riser pipe is used to assess the void fraction evolution in the system and to obtain a three-dimensional visualization of the transient flow during flashing. The flow pattern is observed to transition between bubbly and slug/churn regimes.

Bakhmet'ev et al. (2009) performed large-scale experiments representing the PCCS of the WWER-1200 reactor. Tests were performed to evaluate its performance at heat loads ranging from 0.5 to 1.8 MW. The onset of mass flow, as well as temperature, and pressure oscillations are observed in the riser tubes due to steam formation (due to saturation conditions) as water in the downcomer attained a critical temperature of 70 °C at 1.8 MW load. Oscillations stabilized as water in the tank got heated to 100 °C. Upon further decrease in heat load to 0.5 MW, flow oscillations are again observed with flow rates from 12 to 25 kg/s. Upon assessing the results, it is recommended to decrease the heat exchanger surface area to obtain optimal performance.

Kumar et al. (2012) performed tests in a parallel channel natural circulation test facility (PCNCTF) to simulate the thermal–hydraulic behavior of an advanced heavy water reactor during start-up and during part- or full-power operation. A combination of vertical and inclined riser tubes are used to perform single-phase pressure drop and two-phase natural circulation tests at different pressures up to 70 bar and with varying degree of inlet subcooling. Results from the tests point to the existence of Type-I, Type-II stability boundaries, and stable two-phase zones which were numerically simulated and predicted using RELAP5/MOD 3.2 code.

Cloppenborg et al. (2014) performed experiments to investigate the thermal-hydraulics of single- and two-phase flow regimes encountered in passive safety systems in a generic test facility called GENEVA. The impact of downcomer and riser geometries on the resulting flow behavior and its instabilities are investigated using void fraction and temperature sensors installed at different locations along the riser tubes. It is observed during two-phase flow instabilities that a high void fraction results in high mass flow amplitudes due to decrease in hydrostatic pressure along the riser. Flashing and flow reversal in the riser tube are observed during experiments.

AREVA (Wagner and Leyer, 2015; Leyer et al., 2010) performed a full-scale testing of KERENA's PCCS at the INKA (Integral Test stand Karlstein) facility with the aim of determining the heat transfer capacity as a function of (a) pressure in the flooding pool vessel, (b) pool temperature, and (c) concentration of non-condensable gases. Coolant water in the PCCS transitioned from a single-phase flow at the start of the test (0–1500 s) to a two-phase oscillatory flow during the middle of the test (1500–2500 s) and attaining a stable flow circulation with high coolant temperature towards the end of the test (2500–6200 s). Results showed that up to 7 MW heat is transferred to the PCCS.

Hou et al. (2016) performed a series of tests to expand upon and understand the mechanisms related to the initial observation of a type of flashing instability induced water hammer in one of the tests in a PCCS test facility. It is observed that the long horizontal tube at the lower part of the riser induces water hammer effects due to the periodic violent evaporation and condensation taking place there. The effect of parameters such as the condenser tube outlet temperature, the inlet subcooling, the loop structure, and the presence of non-condensable gas components are studied to mitigate the water hammer effects. Based on the results, a flow regime map describing the scope and intensity of the water hammer effects is created.

Shi et al. (2015) performed tests to study start-up transients in a scaled BWR type reactor known as Purdue Novel Modular Reactor (NMR). Normal (0.5 bar, 18 °C at core inlet) and pressurized (3 bar, 53 °C at core inlet) transient tests are done at the NMR with a vertical riser tube configuration to assess thermal–hydraulic parameters like system pressure, coolant flow velocity, and distribution of local void fraction. Instabilities such as flashing and density wave oscillation are observed at system pressure below 5 bar. No such instabilities are observed during the pressurized start-up procedure.

Xiaofan et al. (2017) performed tests to study flow instabilities induced in a natural circulation system to assess it from the perspective of flashing and boiling processes. Tests are performed with a vertical riser setup at atmospheric pressure and at temperatures between 60 and 99.2 °C. Six modes of two-phase flow in the open circulation loop is observed, namely, (i) geysering, (ii) flashing, (iii) compounded flashing, (iv) steady flashing, (v) boiling instability, and (vi) steady boiling flow. Parametric studies are performed by varying the riser length and flow friction coefficient, heating power, inlet subcooling. Besides, tests to study air injection into riser tubes on the formation of steady flashing flow is performed and it is observed that boiling instability acts as an interference on steady flashing flow.

Tompkins and Corradini (2018) performed tests at 1 bar in a two-phase flow natural circulation facility to assess the performance of reactor cavity cooling systems for Generation IV reactors. WMS instrumentation is installed in three adiabatic vertical risers to assess void fraction and flow instabilities. A transition from stratified to intermittent flow regimes is observed during tests as water inventory in the storage tank is reduced due to evaporation. It is accompanied by oscillatory flow rate due to fluctuating pressure drops between the flow regimes confirming the presence of a flow transition instability.

There is a dearth of experimental literature discussing the flow dynamics related to flashing and geysering in an external condenser PCCS. Specifically, the effect of condenser tube inclination on the ensuing flow dynamics has not yet been systematically investigated although different inclinations are used in commercial designs. Examples include the vertical condenser tubes used in HPR1000 and VVER-1200 reactors and the inclined (angle unknown) condenser tube design used in AHWR and KERENA reactors. While results from steam condensation experiments (Jeon et al., 2015a, Jeon et al., 2015b) on the primary side of the PCCS demonstrate that a lower condenser tube inclination produces higher heat transfer coefficients over higher inclination tubes by

15–30 %, corresponding studies on the flow dynamics within the secondary side of the PCCS are still lacking. Another reason to study this issue is to expand the scope of external condenser PCCS experiments to include the condenser tube inclination effects to validate the existing observations (Jeon et al., 2014) regarding its favorable long-term cooling performance. The aim of this study, therefore, is to discuss the details of a test facility at the University of Luxembourg (UL) dedicated to condenser tube inclination studies and to present the preliminary test results from this facility.

2.1. Experimental facility

The special purpose test facility at the UL to study the flow dynamics and instabilities in an external condenser PCCS design is called INTRAVIT. It is an acronym for INvestigation of passive heat TRAnsfer in a Variably Inclined Tube. The facility comprises four major components: an overhead pool, a downcomer tube, a variably inclined condenser tube, and a riser tube, respectively as shown in Fig. 3.

The pool (2.9 m × 0.78 m × 1.005 m) is installed at the top of the facility and its walls are made of transparent, polycarbonate plates. This design enables a visual observation of the collapsing vapor bubbles inside the pool during the instabilities. Deionized water is used as the working fluid in the INTRAVIT facility. There is a 20 kW heater placed in the pool to heat up the fluid to a pre-defined temperature prior to starting the experiments. At the same time, a 66 kW heat exchanger is also installed in the facility to cool down the fluid temperature in the pool to a desired value prior to starting certain experiments.

The downcomer (Material: Stainless Steel 1.4404) line begins with a Krohne Optimass 1000–S 15 Coriolis mass flow meter. Form loss coefficient through the mass flow meter is estimated based on the data sheet provided by the manufacturer. The formula used is

$$K = \frac{\Delta P}{2\rho U^2}$$

Where K – Form loss coefficient, ΔP – Pressure drop (Pa), ρ – Fluid density (kg m^{-3}), U – flow velocity (m/s). The value of K varies between 1.4 (at max. flow rate of 1.8 kg/s) and 5.5 (at min. flow rate of 0.01 kg/s).

The mass flow meter is followed by a fixed pipe of length 600 mm with an inner diameter of 24 mm. After the fixed pipe is an adjustable pipe with an outer and inner diameter of 18 mm and 16 mm, respectively. This pipe is modular in design and is placed within the fixed pipe

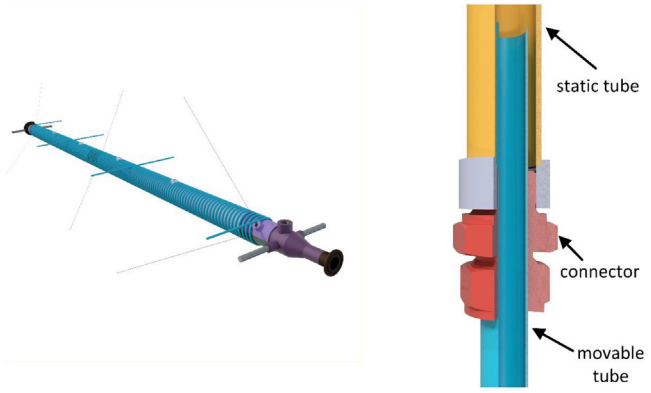

Fig. 4. Left: drawing of the condenser tube. Heating wire marked in blue. Right: Section view of the connection of the static and the movable downcomer tube.

to adjust the length of the downcomer line in response to the varying inclination of the condenser tube during experiments.

The end of the adjustable pipe in the downcomer line is connected to a variably inclined condenser tube (Material: Stainless Steel 1.4404, length – 1400 mm, inner diameter – 34 mm) through a diffuser component to avoid any adverse flow effects (e.g. detachment, turbulence etc.) during the experiments. During nuclear accidents, the heat-up of coolant inside a PCCS condenser tube occurs in a non-uniform manner along its cross-section and over its length due to uncontrolled release of steam into the containment. But it is desirable in lab-scale tests to have a uniform and controlled heating of coolant in the condenser tube over the entire length for (a) repeatability of experiments and (b) providing accurate inputs to develop and validate numerical models. Thus the unique feature of INTRAVIT facility is the electrical heating system to heat-up the fluid flowing inside the condenser tube. Three electrical heating wires (each 6 m length with 3.2 mm diameter as shown in Fig. 4) are wound around the condenser tube over a length of 1200 mm to achieve uniform heating. Each heating wire has a maximal power of 1320 W so that the total heating power sums to 3960 W.

The connection between the downcomer line and the condenser tube enables different condenser tube inclinations to be realized starting from 0° (horizontal position) to 90° (vertical position). With increasing angle, the downcomer-condenser tube connection moves downwards (see Fig. 5) and in effect the position of the riser tube has to

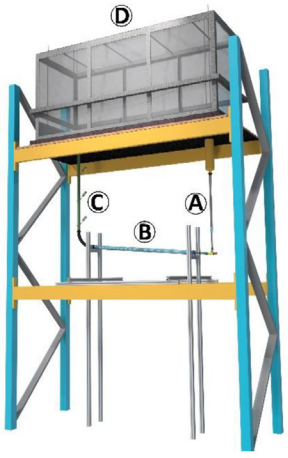

Fig. 3. Overview of the INTRAVIT test facility. Left: CAD drawing, A: downcomer tube, condenser tube, C riser tube, D tank. Right: Photo of INTRAVIT.

Fig. 5. Different inclination angles of the condenser tube: left – 5°, middle – 60°, right – 90°.

be shifted forward towards the downcomer. There are 9 flange connections located at the bottom of the pool between the riser and downcomer to enable the forward shift in riser during rising condenser tube inclination as shown in Fig. 5.

The final part of the INTRAVIT facility that completes the coolant loop is the riser tube (Material: Stainless Steel 1.4404). A flexible metal hose at the end of the condenser tube is used to connect to one end of the vertical riser tube (length – 1000 mm, inner diameter – 34 mm). The other end of the riser tube is connected to the pool. In general, the form loss coefficients through the pipes and piping connections shall be estimated using the standard formulae for pipe flows in literature (Rennels and Hudson, 2012).

3. Instrumentation

Table 1 shows the different instrumentation installed in the INTRAVIT facility to obtain quantitative information of the flow dynamics during the measurements. To start with, the pool is instrumented with 26 thermocouples at different heights spread around its entire volume. A Coriolis mass flow meter is installed at the beginning of the downcomer line and a low-frequency (1 Hz) thermocouple is installed at the end of the downcomer line to record the mass flow and temperature, respectively. The condenser tube is instrumented with 18 wall thermocouples (9 on the outer wall and 9 on the inner wall) and 2 relative pressure sensors (1 at the inlet and 1 at the exit). Besides, 6 thermocouples are installed in the bulk of the flow at 280 mm intervals over the entire length of the condenser tube. The positioning of the measurement points are show in Fig. 6.

The 18 wall thermocouples in the condenser tube are installed in three separate sections spaced 500 mm apart along the condenser tube. In each section, the pipe is cut in two-halves (marked red and green in Fig. 7) to install 6 thermocouples (3 on the outer wall and 3 on the inner wall) over a section length of 66 mm. The angle between thermocouples is 120° and the inner wall thermocouples are placed in a groove, then soldered and grinded to prevent any flow disturbances as shown in Fig. 7. This section is then welded to the condenser tube and the same process is applied for the other two sections as well.

Since two-phase flow instabilities such as flashing and geysering is expected to occur along the riser tube, it is instrumented with 4 thermocouples and 3 needle probe sensors to measure the local temperature and void fraction, respectively. The operating principle of a needle probe sensor is described in Prasser et al. (2002). The tips of the thermocouple and the needle probe are 5 mm apart at each location as shown in Fig. 7. The needle probes are positioned at an angle of 45° into the bulk so that the oncoming bubbles (during flashing and geysering) could be easily penetrated by the probes. The first riser thermocouple is installed at 52 mm from the riser inlet. Further three measuring positions are spaced at 300 mm intervals along the length of the riser tube.

3.1. Experimental procedure

The execution of all the experiments at the INTRAVIT facility are carried out at steady-state boundary conditions with a pre-determined condenser tube inclination and pool temperature. The following procedures are carried out prior to the experiments

- The condenser tube is brought to the required inclination manually by lowering the condenser tube-downcomer line connection.

Table 1
Overview of the instrumentation.

Component	Instrumentation	Error	No. of sensors	Recording Frequency (Hz)
Pool	Thermocouple (Type T)	± 0.43 °C	26	1
Downcomer	Coriolis mass flow meter	± 0.11%	1	10
	Sheath thermocouple (Type T, 1 mm)	± 0.29 °C	1	1
Condenser tube	Sheath thermocouple (Type T, 1 mm)	± 0.29 °C	6	1
Condenser tube – Inner wall	Sheath thermocouple (Type N, 0.5 mm)	± 0.97 °C	9	1
Condenser tube – Inner wall	Sheath thermocouple (Type N, 1 mm)	± 0.97 °C	9	1
Condenser tube	Pressure Transducer	0.1%	2	10
Electrical heating wire	Sheath thermocouple (Type N, 1 mm)	± 0.97 °C	3	2
Riser tube	Sheath thermocouple (Type T, 1 mm)	± 0.29 °C	4	2
	Coaxial needle probe sensor (2 mm)	–	3	1000
Ambient	Type K thermocouple	± 1.0 °C	1	1

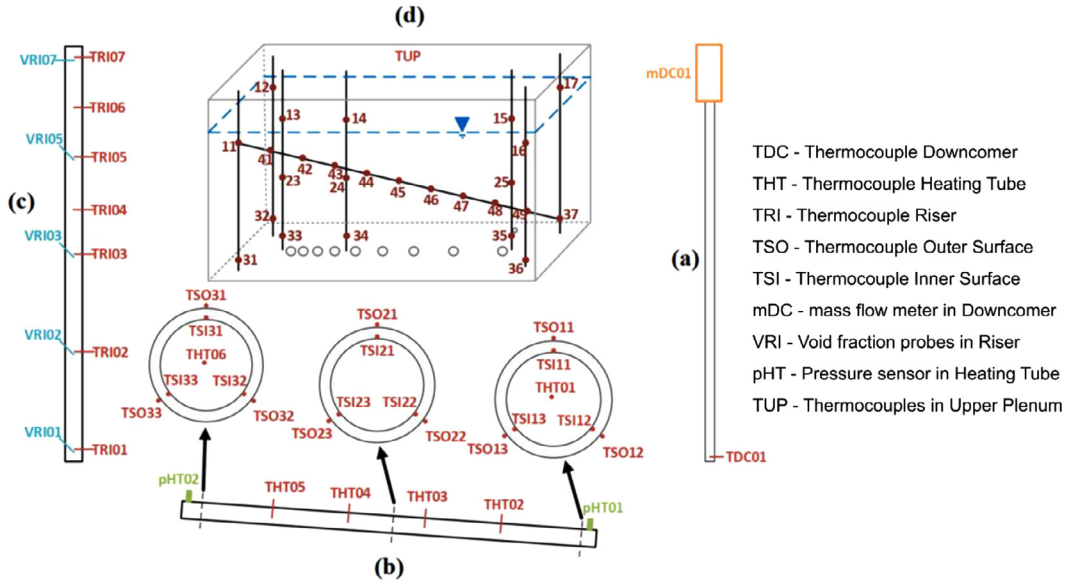

Fig. 6. Instrumentation in (a) down comer - DC tube, (b) heating tube - HT, (c) riser tube and (d) pool. Red: Thermocouple, Blue: void fraction probe, Green: relative pressure sensor,

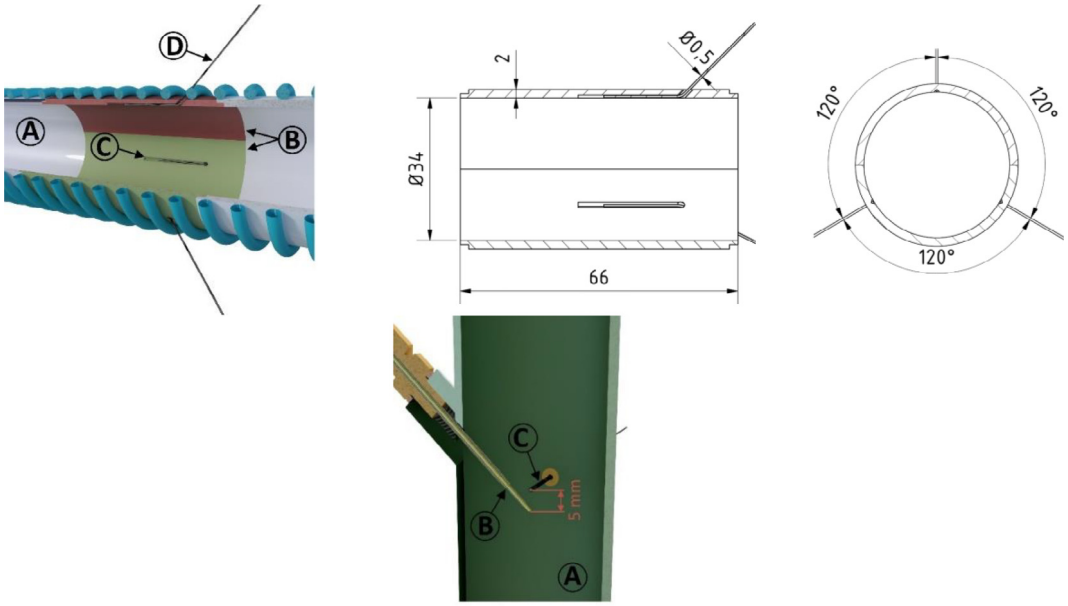

Fig. 7. Top – Section view and technical drawing of the positioning of the inner wall thermocouples. A: condenser tube, B: 2 tube sections, C: groove, D: thermocouple section; Bottom – View of the riser tube (A) with the needle probe (B) and the thermocouple (C).

- The heater in the pool is then switched on to bring the fluid to a desired temperature. Thermocouples in the pool are used to monitor the temperature evolution.
- At the same time, electrical heating is switched on and is set to 20% of its maximum power to warm the structure of the condenser tube.
- This process lasts between 40 min and 95 min depending on the desired temperature and the overall fluid temperature in the INTRAVIT facility is gradually raised.

Once the fluid in the pool attains the preset temperature, experiment begins and the procedure is described as follows

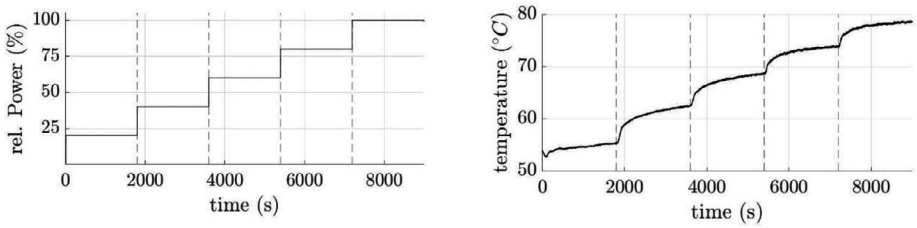

Fig. 8. Illustration of power profile of the electrical heater (left) and the corresponding temperature response (right) during measurements.

- The heater in the pool is switched off.
- Electrical heating power is kept at 20% of its maximum power for a period of 30 min.
- Electrical heating power is then raised to 40% of its maximum power and is kept at that level for a period of 30 min.
- Likewise, the heating is stepped up to 60%, 80%, and 100% while keeping a time period 30 min at each power level. An illustration of the electrical heating and the corresponding temperature increase during the measurements is shown in Fig. 8.
- Whether single-phase or two-phase natural circulation flow is established in the loop is a function of (a) starting temperature in the pool, and (b) the condenser tube inclination.
- Data from all the sensors recorded during the entire process are saved to a local workstation at the facility.
- Once the test is completed, the electrical heating is switched off. The fluid temperature in the pool is reduced by circulating it (using a pump) through a heat exchanger. For the next set of tests, the aforementioned processes are repeated.

3.2. Execution of experiments and data acquisition

Experiments are executed and controlled using the National Instruments (NI) systems engineering software called LabVIEW (Laboratory Virtual Instrument Engineering Workbench). The graphical layout of the INTRAVIT facility in LabVIEW is shown in Fig. 9. Based on a producer–consumer structure, three producer loops (loop # 1–3) in LabVIEW acquire data from three different input tasks and data in each loop is inserted to a queue. At the same time a consumer loop (loop #4) in parallel checks the length of each queue and empties the queue with most waiting elements and writes the output data reducing data congestion. There exists another loop (loop #5) whose function is to compare the current temperature of the heating wire to its predefined maximum temperature and switches it off in case of overheating. User interaction and live data (e.g. temperature, mass flow) during measurements is performed by a separate loop (loop #6).

All the sensors provide an analog signal. The mass flow meter provides a current output which is transformed in the control box to a voltage output. The pressure and temperature sensors deliver a direct voltage output. An NI-9214 module is used to measure and acquire low-speed thermocouple data at 1 Hz frequency while an NI-9212 module is used to measure and acquire high-speed thermocouples at 2 Hz frequency. Voltage data for pressure and mass flow meter is measured and sampled at 100 Hz by the NI-9205 module before converting it to 10 Hz by averaging every 10 samples to reduce the data size. Voltage control for the heating wires is provided using an NI-9263 module while an NI-9481 relay module is used to switch on the heating wires on the condenser tube and the heater in the pool. All the above modules are connected to an NI-9178 chassis that allows 4 tasks to be executed in parallel of which one is used for the low-speed thermocouples (1 Hz), one for the high-speed thermocouples (2 Hz), one for the voltage input (1000 Hz) and one task that is used for the signal output. Data from the chassis is transferred to the local workstation via a USB connection.

The local void data are recorded using a data acquisition system provided together with the software for operation and post processing by the Helmholtz Zentrum Dresden Rossendorf (HZDR) institute in Germany. The data acquisition frequency is 1000 Hz. During the post processing, 10 data samples are averaged, so that the resulting frequency is 100 Hz.

Table 2
experimental matrix.

Test #	Condensation tube inclination (°)	Fluid temperature in the pool (°C)
1	5	50
2	60	50
3	90	50
4	5	85
5	60	85
6	90	85

4. Results

The first test results from the INTRAVIT facility are discussed in this section. 6 tests are performed with three different condenser tube inclinations and two pool temperature combinations as shown below in the test matrix provided in Table 2. Tests 1–3 represent the early stage of a PCCS operation with a pool temperature of 50 °C while tests 4–6 represent the late stage PCCS operation with a pool temperature of 85 °C.

Among the different data collected during the tests, the following parameters are used to describe the fluid flow dynamics observed during the tests 1–6:

- Mass flow – to describe fluid circulation under normal (single-phase) and unstable (two-phase) flow conditions,
- Fluid temperature difference (ΔT) between the inlet and the exit of the condenser tube – to assess the heat transferred from the electrical heating system to the fluid,
- Temperature and void fraction in the riser – to characterize the state of the fluid during its upward motion, and
- Pool temperature – to assess the evolution of heat transfer coming from the heat source (inclined condenser tube)

4.1. Tests 1–3

Fig. 10 shows the temporal evolution of mass flow and ΔT for tests 1–3 at inclination angles of 5° (α05T50), 60° (α60T50), and 90° (α90T50). An increase in the mass flow and ΔT in the coolant loop are observed during the ramp-up of the electrical heating from 20% to 100%. At any given instant, a higher fluid mass flow is observed with

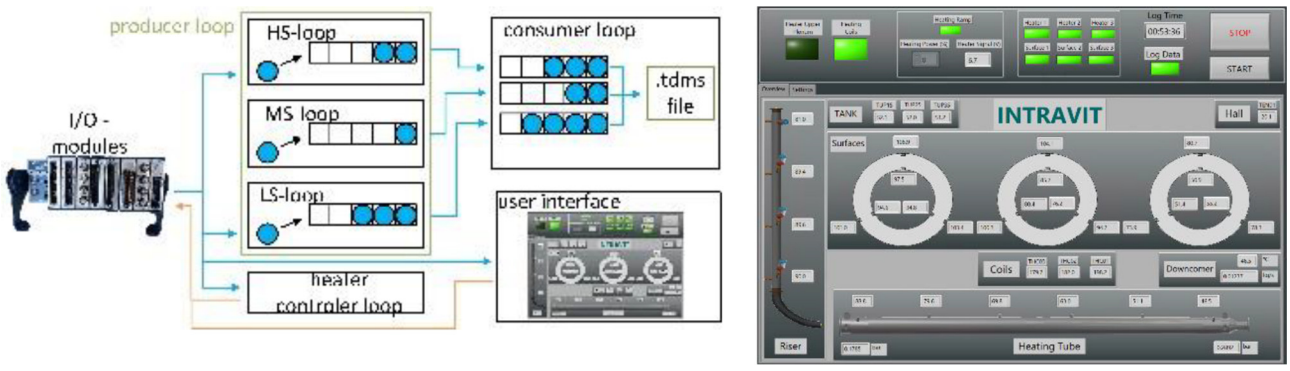

Fig. 9. left: Loop structure of the LabVIEW program. Right: GUI.

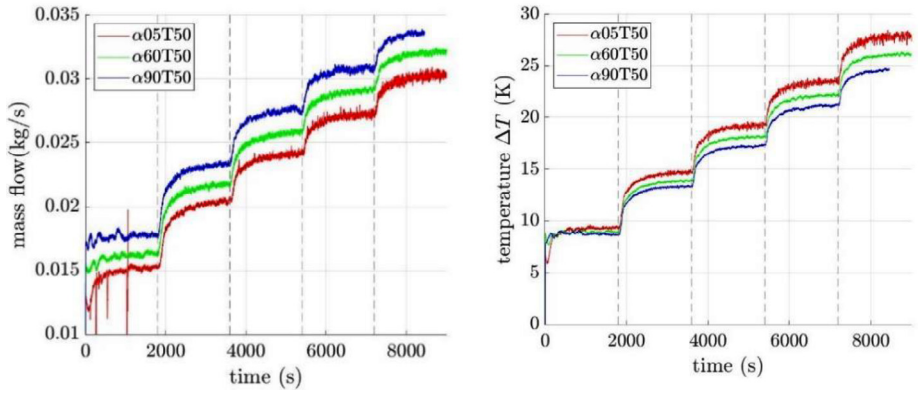

Fig. 10. Mass flow (left) and temperature difference (ΔT) between the inlet and exit of the condensation tube (right) at T_{pool} = 50 °C.

higher condenser tube inclination due to buoyancy. With rise in inclination, it becomes easier for the flow to move upwards due to strong buoyancy forces causing an overall increase of mass flow in the system. This results in a lower fluid ΔT between the inlet and exit of the condenser tube with rising inclination, also shown in Fig. 10, due to the interplay of the following factors

(a) At same heating power (Q), ΔT is inversely proportional to the mass flow (m) as dictated by the principle of energy balance ($Q = m.C_p.\Delta T$), and
(b) increased single-phase heat transfer coefficient (h) across the cross-sectional area (A) caused by the reduction in ΔT according to Newton's law of cooling ($Q = h.A.\Delta T$)

Fig. 11 shows the temperature contour plot for tests 1–3 at 100% heating power. Data from 11 thermocouples, located in the bulk flow, are used to construct this contour plot. Of these 1 is located at the end of the downcomer line, 6 in the condenser tube, and 4 in the riser. The primary Y-axis denotes the length coordinate starting from the end of downcomer line till the top of the riser tube. Fluid mass flow is shown in the secondary Y-axis. It is observed during tests 1–3 that fluid from the downcomer enters the condenser tube at subcooled conditions (50 °C) and gets heated to 80 °C (Test 1), 78.6 °C (Test 2), and 77.8 °C (Test 3), respectively, at the end of the condenser tube. These temperatures remain unchanged as the fluid ascends upward in the riser tube. The stable mass flow pattern points to a single-phase natural circulation phenomenon during all these tests. This argument is also confirmed by the fact that the maximum temperature in tests 1–3 is lower than the saturation temperature (101.76 °C) corresponding to the pressure at the end of the riser tube (1.08 bar). Besides, the needle probe sensors in the riser tube have not detected any vapor bubbles confirming the single-phase flow phenomenon as shown in Fig. 11.

Fig. 12 shows the temperature distribution over the height of the pool at a fixed position on each side of the pool for tests 1–3. Thermocouples at the side of the riser tube are marked T13 (top), T23 (middle), and T33 (bottom), respectively while thermocouples at the side of the downcomer tube are marked T15 (top), T25 (middle), and T35 (bottom), respectively. Starting from 50 °C, a steady rise in fluid temperature occurs in the pool during tests 1 – 3 and becomes nearly 55 °C at the end of the tests. Temperatures of the upper (TUP13 and TUP15) and the middle (TUP23 and TUP25) thermocouples in the pool are much closer relative to the lower thermocouples (TUP33 and

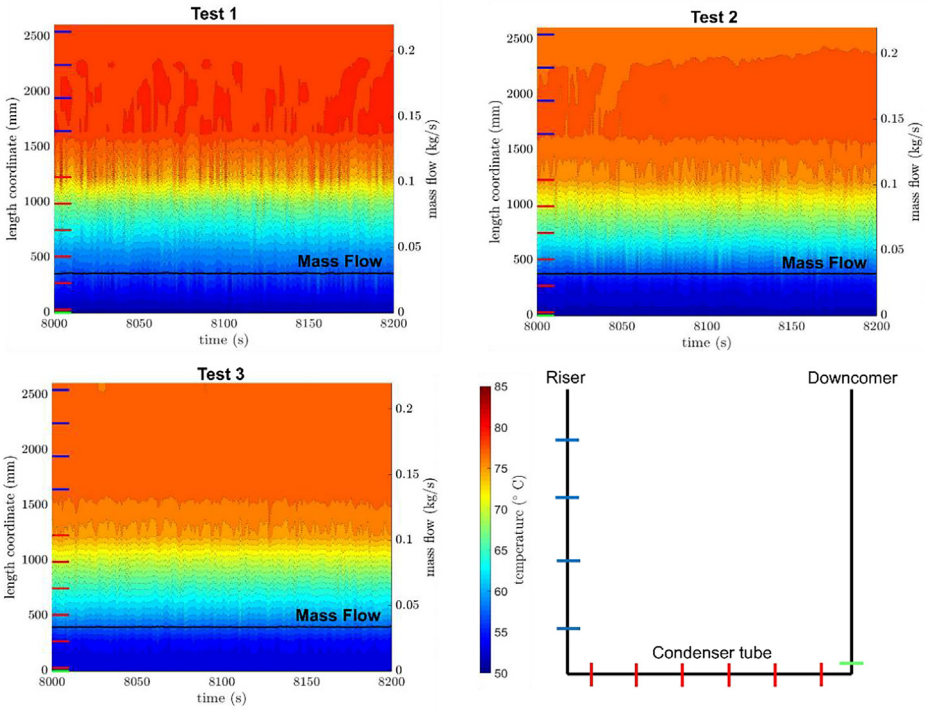

Fig. 11. Temperature contour with overlying mass flow plot for tests 1 – 3 at 100% heating power. Sketch at the bottom right shows the downcomer (green), condenser tube (red), and riser (dark blue) thermocouple data used in the Y-axis (length coordinate) of the contour plot. (For interpretation of the references to colour in this figure legend, the reader is referred to the web version of this article.)

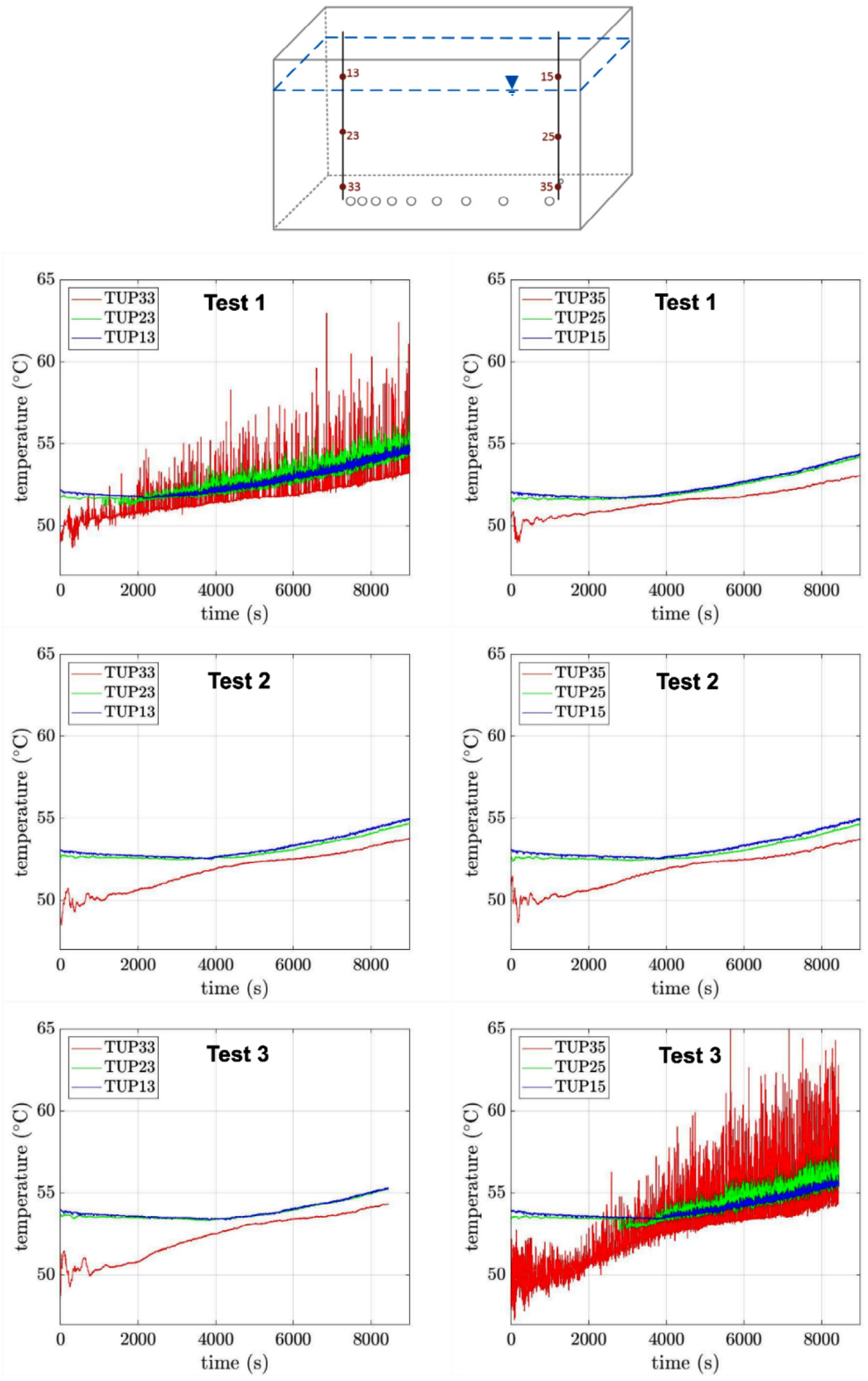

Fig. 12. Vertical temperature stratification on each side of the pool for the tests 1–3.

TUP35). There exists a slight thermal stratification within the pool due to this temperature gradient. Test 1 (Fig. 12(a)) shows strong temperature fluctuations in the pool above the riser tube due to the turbulent mixing of the warm water exiting the riser tube and the cold water of the tank. The same behavior is observed for test 3 (Fig. 12(c)) at the other side of the tank because of the riser is shifted close to the downcomer inlet for 90° inclination of the condenser tube (see Fig. 5). For test 2, the thermocouples are far from the riser outlet, so no fluctuations are observed.

4.2. Tests 4–6

Fig. 13 shows the temporal evolution of mass flow and ΔT for tests 4–6. While a steady increase in the mass flow and ΔT in the coolant loop

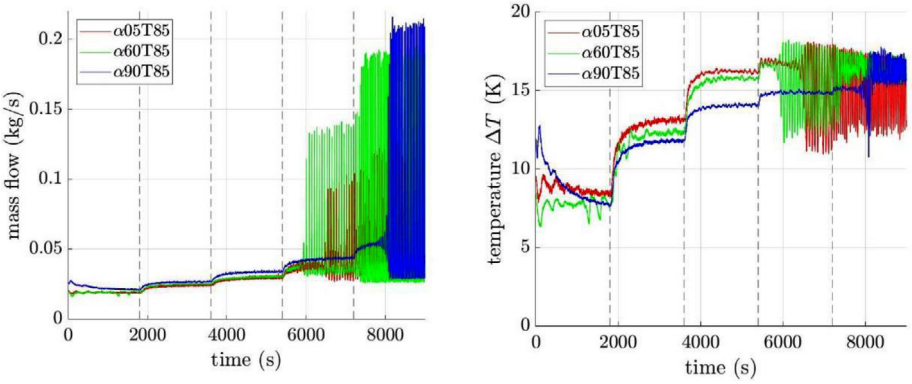

Fig. 13. Mass flow (left) and temperature difference between the inlet and exit of the condensation tube (right) at T_{pool} = 85 °C.

are observed during the ramp-up of electrical heating from 20% to 60%, cyclical mass flow and ΔT oscillations are observed at 80% heating power and get intensified at 100% heating power. This could be inferred as two-phase flow instabilities caused by flashing and/or geysering. Therefore, the flow behavior at 80% and 100% electrical heating power are discussed below separately.

4.2.1. At 80% heating power

Fig. 14 shows the temperature contour and the void fraction data (similar to Fig. 2) at 80% electrical heating power in the condenser tube.

Test 4: Fluid exiting the condenser tube is slightly above 100 °C and begins evaporating as it moves up in the riser tube due to reduced static pressure. This triggers the formation of vapor bubbles which grow in size during its upward motion and flashes out into the pool. The flashing triggered flow instability results in a sudden ingress of fluid mass into the downcomer line as seen from the mass flow peak in Fig. 14(a). After this event, a temporary flow equilibrium is attained as single-phase natural circulation condition is restored. After a certain time interval, the fluid in the condenser tube is heated to near saturation conditions and flashes in the riser tube again. This phenomenon occurs at regular intervals as seen from Figs. 13 and 14(a). The local void fraction data indicates the flashing is not very strong as seen from the sparse distribution of white lines (denoting vapor bubbles) starting from the middle of the riser tube (at y = 2000 mm in Fig. 14(a)).

Test 5: The aforementioned phenomenon is even more strongly observed at 60° inclination of the condenser tube. Flashing in test 5 differs from test 4 in the following aspects:

(i) The magnitude of flashing is much pronounced as seen by a singular mass flow peak (at an average value of 0.14 kg/s) in Fig. 14(b) which is 40% higher than in test 4 (at 0.1 kg/s).
(ii) As the vaporized mass rapidly flashes out into the pool, subcooled liquid from the pool flows into the riser tube as seen from the blue contour near the top of the riser tube (marked 'A' in Fig. 14(b)). This is detected by the top most thermocouple in the riser tube in test 5 while it is not detected in test 4 due to the less intense flashing as shown in Fig. 4(a).
(iii) Void fraction data for test 5 shows strong flashing effect starting from the middle of the riser tube where vapor occupies nearly the entire cross-section during the flashing phenomena in comparison with test 4.

Test 6: At 90° (vertical position) condenser tube inclination, no flashing or two-phase flow behavior is observed from the test data. Mass flow remains constant throughout this period and the temperature contour displays a gradual rise in temperature from the condenser tube inlet till the exit of the riser tube as seen in tests 1–3. Void fraction data also shows no detection of vapor bubbles in the riser confirming the single-phase natural circulation flow in test 6. The vertical orientation of the condenser tube greatly favors the single phase natural circulation causing a high enough mass flow to limit the heat up to temperatures below saturation. Flashing can thus not occur. Thermocouple data in contour plot shows the maximum temperature of the fluid as it exits the condenser tube is less than 100 °C (marked 'B' in Fig. 14(c)) which is not the case in tests 4 and 5.

4.2.2. At 100% heating power

Fig. 15 shows the temperature contour and void fraction data at 100% electrical heating power in the condenser tube during tests 4–6.

Test 4: Fluid in the condenser tube gets heated more rapidly at 100% heating power resulting in more frequent flashing cycles as shown in Fig. 15(a) in comparison to the flashing frequency at 80% heating power. This observation is also confirmed by the void fraction data indicating increased vapor bubble zones in the riser tube. The peak mass flow in the downcomer during the flashing is increased by 20% to 0.12 kg/s at 100% heating power. It is noticed at the end of each flashing cycle that cold fluid penetrates from the pool into the riser tube to such an extent that it is detected by the upper most thermocouple as marked with a blue circle in Fig. 15(a).

Test 5: At 100% heating power, the fluid attains saturation temperature at the end of the condenser tube and starts boiling. This results in the geysering phenomena which, similar to flashing, causes the vapor mass to grow in size along the riser tube and gets rapidly expelled into the overhead pool. The peak mass flow during all the geysering cycles is nearly 0.19 kg/s – a 28% increase relative to the mass flow at 80% heating power.

The void fraction data from all needle probe sensors confirm this fact indicating the presence of a strong and continuous vapor motion along the riser. Following the geysering phenomena, cold fluid from the pool penetrates even longer into the riser tube (see the dark blue temperature contour at the top of Fig. 15(b)) and is detected by the two upper thermocouples.

Test 6: There is a direct transition from single-phase flow at 80% heating power to frequent geysering cycles at 100% heating power in test 6. Geysering, void fraction, and the cold flow penetration in the riser in test 6 follows a pattern similar to what is described above for test 5. The peak mass flow amplitude at 0.21 kg/s.

Fig. 16 shows the temperature distribution in the pool, similar as in Fig. 3, for the tests 4–6. Tests 4 and 6 show also here strong thermal fluctuations because of the hot water from the riser tube. Due to the flow instabilities caused by the geysering phenomenon, an increase in thermal fluctuations is observed for test 6 for TUP15 and TUP25 starting from t = 8000 s (see video of bubbles entering the pool in attachment).

Compared to the temperature stratification of tests 1–3, the overall stratification is decreased because of the mixing of the water caused by the higher mass flow from the riser tube into the pool. The overall flow

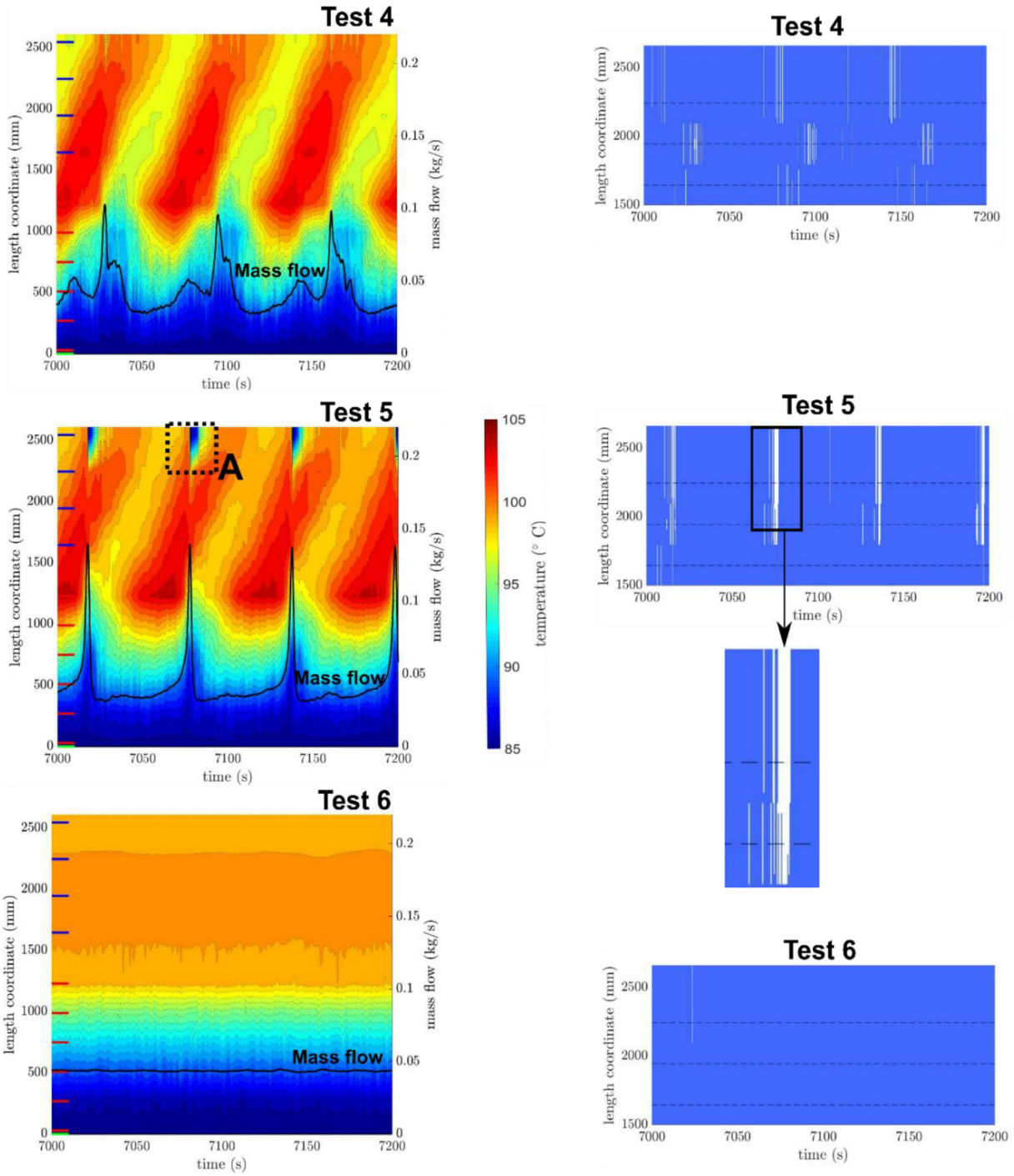

Fig. 14. Temperature contour plot with overlying mass flow plot and local void contour plots (1- needle probe locations are indicated by dotted lines; 2 – White line: Steam, Blue: Water) for the tests 4 – 6 at pool temperature of 85 °C and 80% heating power. (For interpretation of the references to colour in this figure legend, the reader is referred to the web version of this article.)

behavior during each heating phase is summarized below in Table 3. Videos of the flashing phenomenon within the riser and the vapor bubble expulsion into the pool are provided as supplementary animation files.

5. Conclusion

The present paper discusses the flow dynamics taking place in the secondary coolant side of an external condenser PCCS. To this effect, a special purpose test facility named INTRAVIT is built at the University of Luxembourg to perform tests at different condenser tube inclinations between 5° and 90°. The main components of the facility include an overhead pool, a downcomer tube, a condenser tube, and a riser tube. The pool is equipped with a heater to adjust its temperature to start tests at different temperatures mimicking the different stages of an accident. The condenser tube is heated using an electrical heater to reproduce the steam heating in actual accident scenarios. Thermocouples, needle probes, and mass flow sensors installed in the facility are expected to provide a detailed quantitative description of the natural circulation flow encountered during experiments. 6 tests with combinations of two different pool temperatures (50 °C and 85 °C) and three condenser tube inclination (5°, 60°, and 90°) are performed

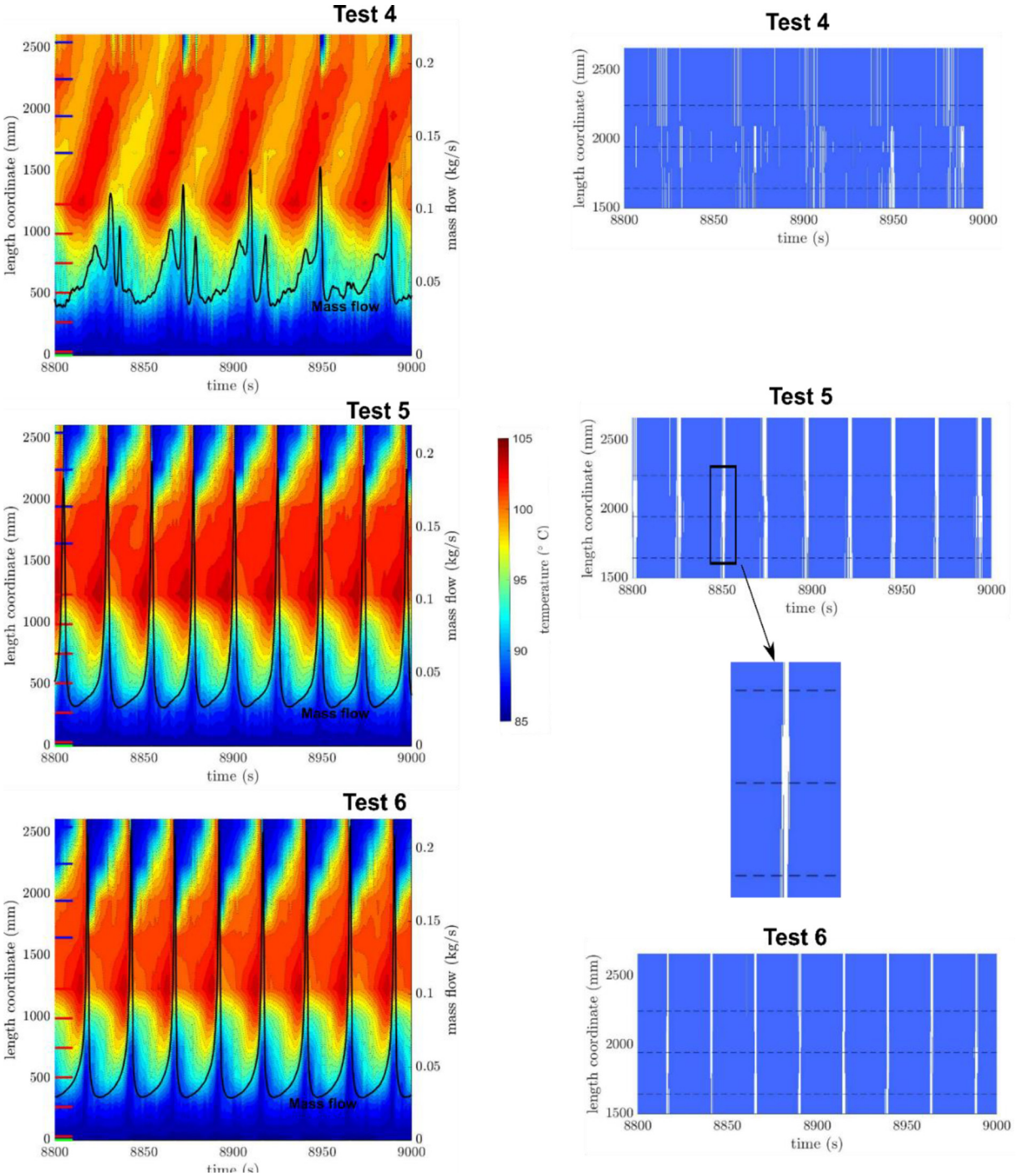

Fig. 15. Temperature contour plot with overlying mass flow plot and local void contour plots for the tests 4–6 at pool temperature of 85 °C and 100% heating power.

and the results could be summarized as follows.

For tests with 50 °C pool temperature, single-phase flow occurs regardless of the condenser tube inclination at 5°, 60°, and 90°. This is because the circulating fluid does not attain saturation temperatures even after getting heated in the condenser tube. High mass flow occurs with rising inclination of the condenser tube due to the effect of buoyancy force. At the same time, ΔT between the inlet and exit temperatures of condensation tube decline with rising inclination due to less time available for heating the flow induced by the high mass flow rates.

For tests at 85 °C pool temperature, flashing behavior is observed during the upward fluid motion in the riser tube at condenser tube inclinations of 5° (at 80% heating power) and 60° (at 80% heating power) while geysering behavior is observed at 90° condenser tube inclination at 100% heating power. This is confirmed by the needle probe and mass flow sensor data. Tests at 60° and 90° inclination with 100% electrical heating power causes fluid boiling in the condensation tube resulting in the geysering phenomenon during the upward fluid motion in the riser tube. It is observed that both flashing and geysering phenomena induce strong vibrations in the riser tube along with the flow instability in the coolant loop. The pool temperature during the tests displayed thermal stratification. Besides, strong flow currents are visually observed during the two-phase flow instabilities such as flashing and geysering.

More tests are planned in the future involving a wide range of condensation tube inclination and pool temperature combinations to

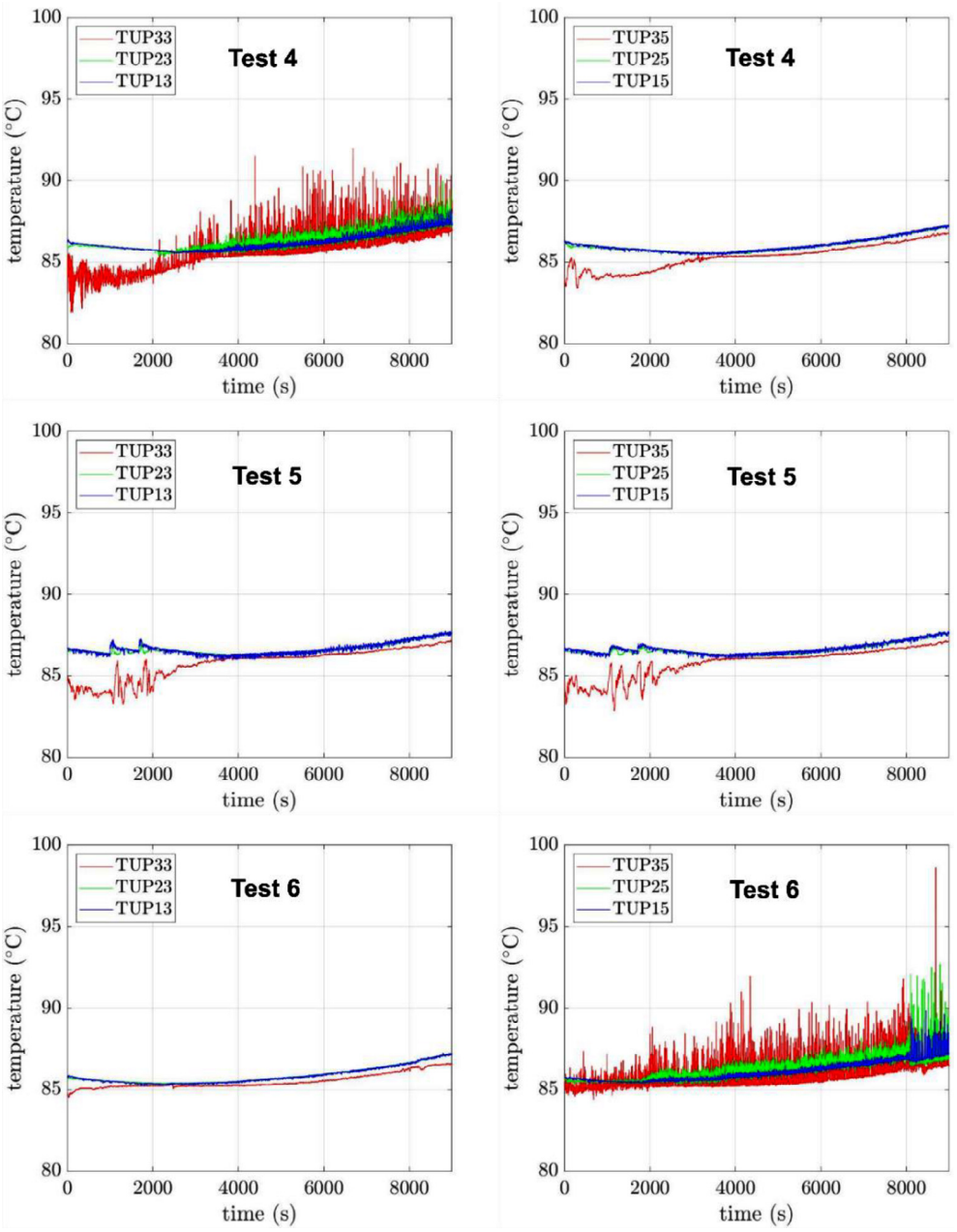

Fig. 16. Vertical temperature stratification on each side of the pool for the tests 4–6.

Table 3
Summary of the flow behavior for test 4–6 at 85 °C pool temperature.

Condenser tube inclination, α (°)	Power (%)				
	20	40	60	80	100
5	Stable	Stable	Stable	Flashing	Flashing
60	Stable	Stable	Stable	Flashing	Geysering
90	Stable	Stable	Stable	Stable	Geysering

assess the effect of single- and two-phase flow dynamics taking place in the INTRAVIT facility representing the external condenser PCCS design. This, along with the planned three-dimensional Computation Fluid Dynamics simulations shall provide a detailed qualitative and quantitative description of the flow phenomena and its effect on the heat transfer process.

CRediT authorship contribution statement

Michel Haag: Conceptualization, Formal analysis, Investigation, Data curation. **P. Karthick Selvam:** Supervision, Writing - original draft, Writing - review & editing. **Stephan Leyer:** Project administration, Supervision, Funding acquisition.

Declaration of Competing Interest

The authors declare that they have no known competing financial interests or personal relationships that could have appeared to influence the work reported in this paper.

Acknowledgements

The authors would like to sincerely acknowledge the contributions from our research partners Prof. Dr. Hans-Josef Allelein and Ms.

Rebekka Gehr from RWTH Aachen in providing technical inputs and partial funding to set up the INTRAVIT test facility.

References

Bakhmet'ev, A.M., Bol'shukhin, M.A., Vakhrushev, V.V., Khizbullin, A.M., Makarov, O.V., Bezlepkin, V.V., Semashko, S.E., Ivkov, I.M., 2009. Experimental validation of the cooling loop for a passive system for removing heat from the AES-2006 protective envelope design for the Leningradskaya nuclear power plant site. At Energy 106, 185–190.

Bezlepkin, V.V., Zatevakhin, M.A., Krektunov, O.P., Krylov, Y.V., Maslennikova, O.V., Semashko, S.E., Sharapov, R.A., Efimov, V.K., Migrov, Y.A., 2014. Computational and experimental validation of a passive heat removal system for NPP containment with VVER-1200. At Energy 115, 215–223.

Cloppenborg, T., Schuster, C., Hurtado, A., 2014. Generic Experimental Investigations of Thermohydraulic Instabilities With Void Fraction Measurement at Natural Circulation Test Facility Geneva. In: Proceedings of the 22nd International Conference on Nuclear Engineering (ICONE) Prague, Czech Republic, July 7 - 11, 2014.

Dreier, J., Aubert, C., Huggenberger, M., Strassberger, H.J., Meseth, J., Yadigaroglu, G., 1999. The PANDA tests for the SWR 1000 passive containment cooling system. Proceedings of the 7th International Conference on Nuclear Engineering (ICONE) Tokyo, Japan.

Hou, X., Sun, Z., Su, J., Fan, G., 2016. An investigation on flashing instability induced water hammer in an open natural circulation system. Progr. Nucl. Energy 93, 418–430.

IAEA, 1991a. The safety of nuclear power : Strategy for the future, Proceedings of the IAEA conference, September 2–9, 1991. Austria, Vienna.

IAEA, 1991b. Safety Related Terms for Advanced Nuclear Plants, IAEA-TECDOC-626.

IAEA, 2009. Passive Safety Systems and Natural Circulation in Water Cooled Nuclear Power Plants, IAEA-TECDOC-1624.

Jeon, B.G., No, H., C.,, 2014. Conceptual design of passive containment cooling system with airholdup tanks in the concrete containment of improved APR+. Nuc. Eng. Des. 267, 180–188.

Jeon, B.G., Kim, D.Y., ShinNO, H. C., C.W., 2015. Parametric experiments and CFD analysis on condensation heat transfer performance of externally condensing tubes. Nuc. Eng. Des. 293, 447–457.

Kakodkar, A., 2014. Evolution of nuclear reactor containments in India: Addressing the present day challenges. Nuc. Eng. Des. 269, 3–22.

Kumar, P.P., Khardekar, A., Iyer, K.N., 2012. Experimental and Numerical Investigation on a Two-Phase Natural Circulation Test Facility. Heat Transfer Eng. 33, 775–785.

Lee, S.W., Heo, S., Ha, H.U., Kim, H.G., 2017. The concept of the innovative power reactor. J. Nucl. Sci. Technol. 49, 1431–1441.

Leyer, S., Maisberger, F., Herbst, V., Doll, M., Wich, M. and Wagner, T., 2010. Status of the full scale component testing of the KERENATM Emergency Condenser and Containment Cooling Condenser. In: Proceedings of the International Congress on Advances in Nuclear Power Plants (ICAPP), San Diego, CA, USA, June 13-17, 2010.

Liu, H., Todreas, N.E., Driscoll, M.J., 2000. An experimental investigation of a passive cooling unit for nuclear plant containment. Nuc. Eng. Des. 199, 243–255.

Manera, A., Prasser, H.M., van der Hagen, T.H.J.J., 2005. Suitability of drift-flux models, void-fraction evolution, and 3-D flow pattern visualization during stationary and transient flashing flow in a vertical pipe. Nucl. Technol. 152, 38–53.

Prasser, H.M., Zschau, J., Böttger, A., 2002. Anordnung zur Messung der lokalen elektrischen Leitfähigkeit in Fluiden. German Patent Registration 19704609.

Rennels, D.C., Hudson, H.M., 2012. Pipe Flow: A Practical and Comprehensive Guide. John Wiley & Sons Inc:, Hoboken, NJ, USA.

Schulz, T.L., 2006. Westinghouse AP1000 advanced passive plant. Nuc. Eng. Des. 236, 1547–1557.

Shi, S., Schlegel, J.P., Brooks, C.S., Lin, Y.-C., Eoh, J., Liu, Z., Zhu, Q., Liu, Y., Hibiki, T., Ishii, M., 2015. Experimental investigation of natural circulation instability in a BWR-type small modular reactor. Prog. Nucl. Energy 85, 96–107.

Sinha, R.K., Kakodkar, A., 2006. Design and development of the AHWR – the Indian thorium fuelled innovative nuclear reactor. Nuc. Eng. Des. 236, 683–700.

Tompkins, C., Corradini, M., 2018. Flow pattern transition instabilities in a natural circulation cooling facility. Nuc. Eng. Des. 332, 267–278.

Tower, S.N., Schulz, T.L., Vijuk, R.P., 1988. Passive and simplified system features for the advanced westinghouse 600 MWe PWR. Nuc. Eng. Des. 109, 147–154.

Wagner, T., and Leyer, S., 2015. Large Scale BWR Containment LOCA Response Test at the INKA Test Facility. In: Proceedings of the 16th Nuclear Reactor Thermal Hydraulics (NURETH) conference, August 30 – September 4 , 2015, Chicago, USA.

Xiaofan, H., Zhongning, S., Guangming, F., Lu, W., 2017. Experimental and analytical investigation on the flow characteristics in an open natural circulation system. Appl. Thermal Eng. 124, 673–687.

Xing, J., Song, D., Wu, Y., 2016. HPR1000: Advanced pressurized water reactor with active and passive safety. Engineering 2, 79–87.